

Determination of Vortex Burst Location on Delta Wings from Surface Pressure Measurements

Douglas I. Greenwell* and Norman J. Wood†
University of Bath, Bath BA2 7AY, England, United Kingdom

A shape parameter for the vortex-induced upper surface pressure distribution on a delta wing has been derived from a simple two-dimensional potential flow model. For this model the half-width of the suction peak is a function solely of the vortex height above the wing surface. Published experimental data are used to show that this result holds for real delta wing flows at low angles of attack, thus allowing a good estimate of vortex trajectory and strength to be made from surface pressure measurements alone. At higher angles of attack, where the vortex burst region is over the wing, the simple model breaks down; however, the variation in half-width with both chordwise location and angle of attack appears to correlate well with the condition of the adjacent vortex. In particular, the burst point corresponds to an abrupt, well-defined change in half-width. This observation offers an alternative to flow visualization techniques for experimental determination of burst location.

Nomenclature

C_p	= pressure coefficient
$C_{p_{\min}}$	= pressure coefficient at suction peak
c	= root chord
K	= nondimensional angle of attack, $\tan \alpha / \tan \epsilon$
p_{\min}, p_0	= static pressure at suction peak
s	= local semispan
V	= freestream velocity
x	= chordwise coordinate
y	= spanwise coordinate
y_{\min}, y_0	= spanwise location of suction peak
y_v	= spanwise location of vortex core
$y_{1/2}$	= half-width of suction peak
z	= height of vortex core
α	= angle of attack
β	= sideslip angle
Γ	= vortex strength
Γ'	= vortex strength parameter, $y_{1/2}/s \cdot x/c \cdot \sqrt{-C_{p_{\min}}}$
ϵ	= wing semiapex angle
Λ	= leading-edge sweep
ρ	= density

Introduction

At high angles of attack, the aerodynamics of delta wings are dominated by the trajectory of the vortex burst region. This is particularly true for lateral behavior, where asymmetric bursts induce significant nonlinearities in force and moment characteristics.¹

The measurement of burst location is thus an important part of the investigation of these flow regimes. However, conventional experimental methods are, to some extent, unsatisfactory. Visual measurements depend on observer judgment of burst location, introducing errors of the order of 5% (Ref. 2), while the tests are often carried out at very low Reynolds numbers to facilitate flow visualization. Direct flow measurements require the use of either a physical probe, which may itself affect the burst location,³ or a sophisticated and hence expensive nonintrusive technique such as laser Doppler velocimetry. Further, the oscillatory nature of the burst location⁴ may complicate the interpretation of velocity measurements.

Previous attempts have been made to correlate vortex burst with surface pressure distributions.^{2,5-7} These efforts have concentrated on the behavior of the suction peaks induced by the leading-edge vortices. In general, the variation of $C_{p_{\min}}$ with angle of attack for a given chordwise location is correlated with the vortex state, but no consistent trends have been noted. For example, in one case the burst is followed by a reduction in the rate of change of the peak suction with angle of attack, whereas in another there is a local reduction in suction underneath the breakdown point followed by a recovery as the burst moves upstream. The results presented in Ref. 7 suggest that this difference in behavior may be a function of chordwise location of the pressure measurements. In general, vortex burst is not associated with any abrupt or well-defined change in peak suction. As a result, recent investigations of vortex breakdown have tended to disregard surface pressure variations.

This paper presents an alternative analysis of surface static pressure data, using a shape parameter derived from a simple potential flow model. At low angles of attack this analysis enables an estimate to be made of vortex strength and core trajectory. At high angles of attack, where the vortex burst is over the wing, the position of the burst point may be determined with comparable accuracy to that of flow visualization techniques. In addition, an insight is provided into the structure of the entire burst region.

Flow Model

For a slender wing at low angles of attack the flow may be assumed to be conical, and the problem reduces to a two-dimensional flow in the crossflow plane.⁸ The simplest possible model of the flow induced by a leading-edge vortex is a point vortex over an infinite plane (Fig. 1a), inducing a suction peak as shown. It can be readily shown that the half-width of the pressure distribution is directly proportional to the height of the vortex. In addition, the vortex strength is a function of the half-width and peak suction of the pressure distribution:

$$z = \sqrt{\frac{1}{\sqrt{2}-1}} \cdot y_{1/2}$$

$$\cong 1.5538 y_{1/2}$$

$$\Gamma = \pi \cdot z \cdot \sqrt{(-p_{\min}/\frac{1}{2}\rho)}$$

$$\propto y_{1/2} \cdot \sqrt{(-p_{\min})}$$

Received Nov. 4, 1991; revision received April 28, 1992; accepted for publication May 6, 1992. Copyright © 1992 by the American Institute of Aeronautics and Astronautics, Inc. All rights reserved.

*Research Officer, School of Mechanical Engineering.

†Senior Lecturer, School of Mechanical Engineering. Member AIAA.

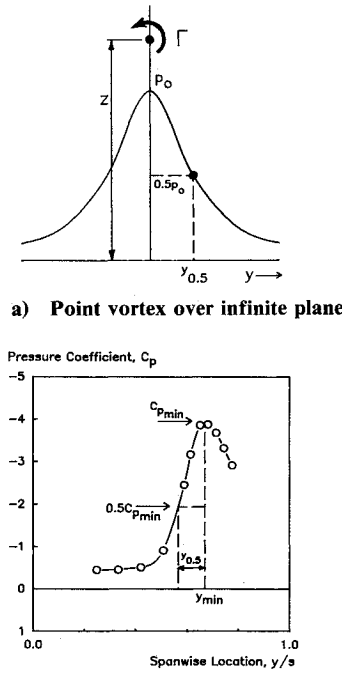


Fig. 1 Definition of half-width for vortex-induced suction peak.

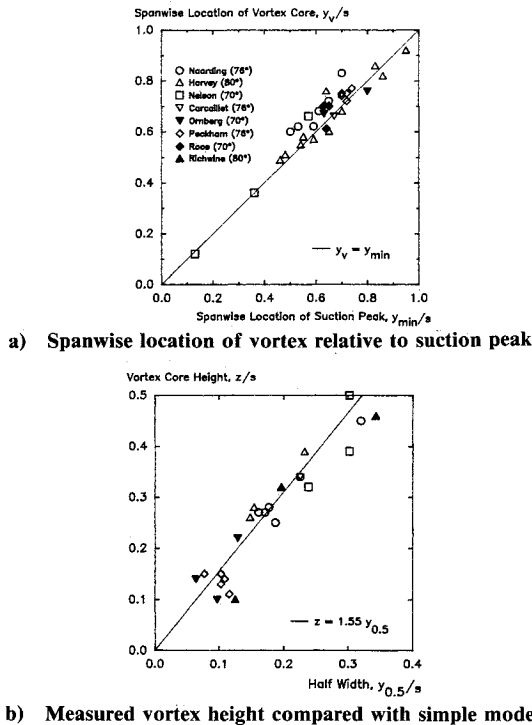


Fig. 2 Application of simple model to experimental vortex trajectory data.

Clearly, a more realistic model would need to take account of the finite nature of the wing, the freestream velocity, the feeding vortex sheet, etc.⁸ However, this would complicate the application of this analysis and tend to obscure the basic physics of the situation. In fact, as will be seen, the simple model gives remarkably good results when applied to experimental data.

Figure 1b shows the definition of half-width as applied to a typical delta wing upper surface pressure distribution.⁷ Although the treatment is in no way rigorous, the justification for this interpretation is that the inner edge of the suction peak

most closely resembles the isolated vortex case, being relatively unaffected by the secondary separation, the leading-edge suction, and the opposite vortex. For ease of application the suction peak is measured relative to a pressure coefficient of zero, rather than the extrapolated asymptote of the pressure distribution curve. Since for low angles of attack the component of freestream velocity in the plane of the wing is close to freestream, the resultant error will be small. For this case,

$$z/s \approx 1.55 y_{0.5}/s$$

$$\Gamma = \pi \cdot V \cdot z \cdot \sqrt{-C_{p_{\min}}}$$

$$= \pi \cdot V \cdot c \cdot (1.55 y_{0.5}/s) \cdot (x \cdot \tan \epsilon/c) \cdot \sqrt{-C_{p_{\min}}}$$

$$\therefore \Gamma/(V \cdot c \cdot \epsilon) \propto \Gamma'$$

where

$$\Gamma' = y_{0.5}/s \cdot x/c \cdot \sqrt{-C_{p_{\min}}}$$

Γ' may be regarded as a vortex strength parameter, and $y_{0.5}/s$ characterizes the shape of the vortex-induced pressure distribution.

A literature search was performed to identify published results containing both vortex core trajectory and upper surface pressure measurements.⁹⁻¹⁸ Figure 2a compares the measured spanwise location of the vortex core and the suction peak. In general, there is good agreement, although for the relatively thick biconvex wing described in Ref. 9 the vortex tends to be around 5% outboard of the suction peak, possibly due to the high spanwise curvature of the wing. Figure 2b shows the measured vortex height plotted against the pressure distribution half-width. The simple flow model can be seen to give a good fit to the data. Figure 3 shows local nondimensional vortex strength (derived from Γ') as a function of Hemsch and Luckring's vortex similarity parameter.¹⁹ Note

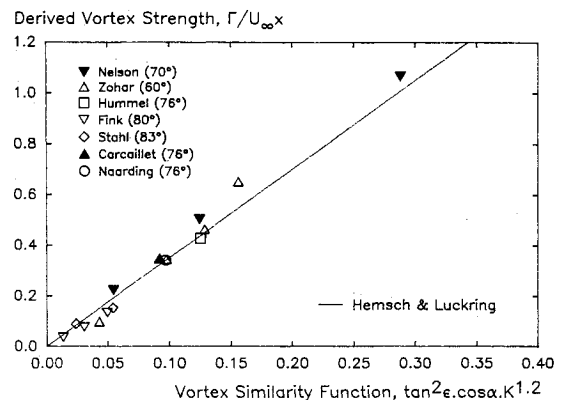


Fig. 3 Vortex strength derived from simple flow model compared with semi-empirical correlation of Ref. 19.

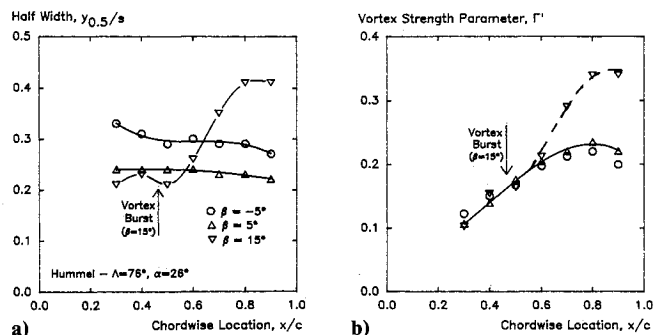


Fig. 4 Chordwise variation of half-width and vortex strength parameter (Ref. 20), showing effect of sideslip and vortex burst.

that only flows approximating to conical behavior (e.g., close to the wing apex) are shown in this figure. A semiempirical correlation from Ref. 19 is also shown.

Although there is some scatter, due in part to the small size and sometimes poor reproduction of the curves analyzed, the simple flow model gives a remarkably good fit. For very high sideslip angles the model breaks down, as the leading-edge effects become significant.

These results encouraged a closer examination of the behavior of the half-width and vortex strength parameter. Figure 4 illustrates the variation of these parameters with chordwise location for a 76-deg delta wing²⁰ at a constant angle of attack. From Fig. 4a it can be seen that for small sideslip angles the nondimensional half-width remains almost constant along the wing, implying a constant nondimensional vortex height, as is indeed the case. The typical upward movement of the leeward vortex with sideslip can also be seen. Similar trends are apparent in data from Refs. 8 and 14. Figure 4b shows the vortex strength parameter increasing linearly from the wing apex as in the classical conical flow assumption, except in the vicinity of the trailing edge. Small sideslip angles have little effect on the vortex strength; this is not immediately apparent from the significantly asymmetric pressure distributions.

It is clear from Fig. 4 that where a burst vortex is present over the wing the simple flow model breaks down. Although the core trajectory is relatively unaffected by the burst, the half-width exhibits a marked increase in the region of the burst, implying a change in the shape of the pressure distribution. This change can also be seen in the vortex strength parameter, which deviates from the "unburst" curve.

Effect of Vortex Burst

Thus, in contrast to the behavior of the suction peak, the half-width of the pressure distribution can change abruptly in the region of a burst vortex. This is confirmed by the analysis of published pressure data^{2,5,8,14} and data from current research work at Bath. These data revealed surprisingly consistent behavior. Figure 5 shows typical variations of half-width with chordwise location and angle of attack, with the burst location marked. In general, vortex burst corresponds to a

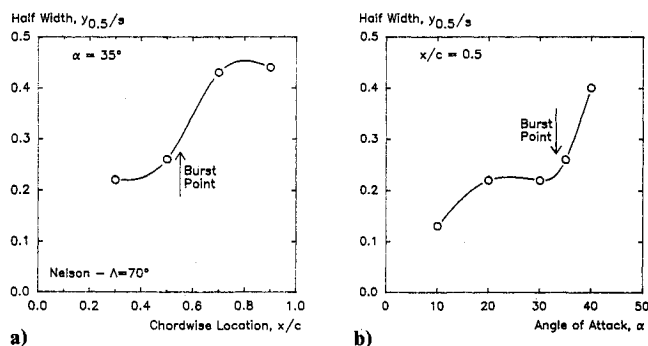


Fig. 5 Typical variation of half-width with chordwise location and angle of attack in the region of the vortex burst (Ref. 2).

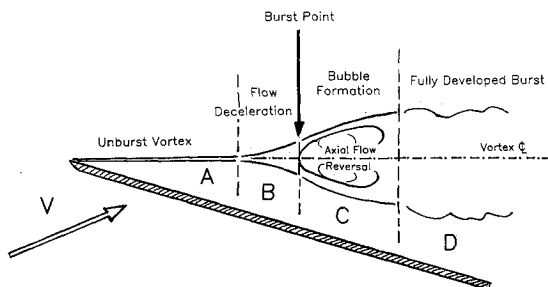


Fig. 6 Schematic of the vortex burst region.

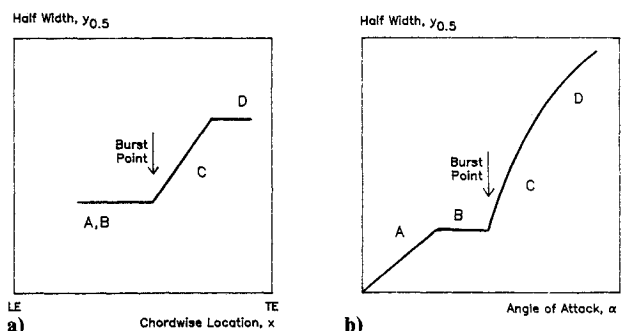


Fig. 7 General half-width trends with chordwise location and angle of attack, related to vortex condition.

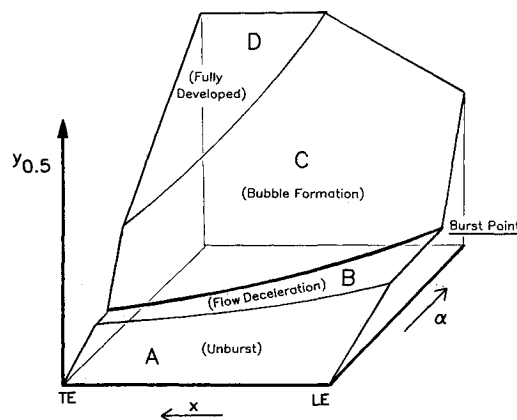


Fig. 8 Proposed interpretation of general half-width trends.

marked, well-defined change in the half-width. If sufficient pressure data are available, the burst location may thus be determined as accurately as with flow visualization techniques.

Inasmuch as half-width is a function of the pressure distribution shape (for constant vortex height), the half-width trends contain considerable information about the vortex breakdown phenomenon.

Figure 6 gives a schematic of the vortex breakdown process split into four regions.^{2,21} Region A denotes the unburst vortex, where the simple model is valid and the half-width is directly proportional to vortex height. Region B indicates flow deceleration ahead of the visible burst point. In the presence of a longitudinal pressure gradient the velocity distribution through an unburst vortex (outside the viscous subcore) gradually changes,^{22,23} such that the swirl component falls off more rapidly with increasing radius. The net effect should be a reduction in half-width. Region C shows a bubble-type breakdown, with some degree of flow reversal in the core. The start of the bubble is usually defined as the burst point, since it is relatively easy to observe. The flow in this region is unsteady and difficult to model; one approach has been to combine a point vortex with a source²⁴ to generate a semi-infinite slender body along the vortex axis aft of the breakdown point, giving a reduction in suction peak and an increase in half-width. The fully developed burst vortex, region D, is often described as a region of large-scale turbulence, although flow visualization indicates that it retains an essentially vortical character.

These stages in the vortex breakdown process may be discerned in the half-width trends typified by Fig. 5. These trends, as synthesized from a wide range of published data, are shown diagrammatically in Fig. 7.

Figure 7a illustrates the general variation of half-width with chordwise location for a constant angle of attack. The difference between the unburst (A) and decelerating flow (B) regions is generally difficult to see on this plot, with half-width remaining essentially constant. Some data sets do show a grad-

ual reduction in half-width from the apex, until the burst point is reached. The burst point, as determined visually, is always in the region of the first kink in the curve. Aft of the burst the half-width increases linearly, as the bubble develops (C), until a plateau is reached when the burst is fully developed (D). This final value is of the order of twice the unburst half-width.

Figure 7b shows the variation of half-width with angle of attack for a given chordwise location. The initially unburst vortex (A) shows a linear increase in half-width and hence height with angle of attack, consistent with observed behavior.²⁵ The curve then levels off, which seems to correspond to the flow deceleration region (B), with a reduced half-width relative to the unburst vortex. The burst point is always in the region of the abrupt increase in half-width at the end of this almost level portion of the curve. The half-width now increases rapidly as the breakdown progresses (C), until the burst is fully developed (D) and the curve approaches a straight line of approximately double the slope of the initial unburst vortex region.

Figure 8 is an attempt to combine the observed half-width trends with both angle of attack and chordwise location in one figure. The shape of the surface will depend on leading-edge sweep and profile.²⁶ The change in half-width at the burst point is most pronounced in the direction of increasing angle of attack.

Conclusions

For an unburst leading-edge vortex, a simple flow model based on a point vortex above an infinite plane gives the result that vortex height is directly proportional to the half-width of the induced pressure distribution on the surface. A surprisingly good match with experimental data is found.

For angles of attack where the vortex burst phenomenon is present over the wing, the burst location is marked by an abrupt change in the half-width of the pressure distributions. There appears to be a good correlation between the various stages of vortex breakdown and the behavior of the half-width parameter.

This observation offers the ability to determine vortex condition and burst location from surface pressure measurements alone. Limitations include the need for extensive pressure tappings and the lack of data on vortex bursts off the wing (i.e., low angle of attack or high sideslip). Conversely, the usual experimental techniques also present considerable practical difficulties, combined with the need for an "eyeball" judgment of burst location.

References

- ¹Lan, C. E., and Hsu, C., "Effects of Vortex Breakdown on Longitudinal and Lateral Directional Aerodynamics of Slender Wings by the Suction Analogy," AIAA Paper 82-1385, Aug. 1982.
- ²McKernan, J. F., and Nelson, R. C., "An Investigation of the Breakdown of the Leading Edge Vortices on a Delta Wing at High Angles of Attack," AIAA Paper 83-2114, Aug. 1983.
- ³Payne, F. M., Ng, T. T., and Nelson, R. C., "Experimental Study of the Velocity Field on a Delta Wing," AIAA Paper 87-1231, June 1987.
- ⁴Portnoy, H., "Unsteady Motion of Vortex Breakdown Positions on Delta Wings," International Council of the Aeronautical Sciences, ICAS-88-6.8.3, Sept. 1988.
- ⁵Zohar, Y., and Er-El, J., "Influence of the Aspect Ratio on the Aerodynamics of the Delta Wing at High Angle of Attack," *Journal of Aircraft*, Vol. 25, No. 3, March 1988, pp. 200-205.
- ⁶Kirkpatrick, D. L. I., "Analysis of the Static Pressure Distribution on a Delta Wing in Subsonic Flow," Aeronautical Research Council, R&M 3619, Aug. 1968.
- ⁷Greenwell, D. I., "Control of Delta Wing Flows at High Angles of Attack," School of Mechanical Engineering Transfer Rept., Univ. of Bath, Bath, England, May 1991.
- ⁸Er-El, J., Seter, D., and Weihs, D., "Nonlinear Aerodynamics of Delta Wing in Combined Pitch and Roll," *Journal of Aircraft*, Vol. 26, No. 3, March 1989, pp. 254-259.
- ⁹Naarding, S. H. J., and Verhaagen, N. G., "Experimental and Numerical Investigation of the Vortex Flow over a Sharp Edged Delta Wing With and Without Sideslip," Delft University of Technology Rept. LR-573, Delft, The Netherlands, Dec. 1988.
- ¹⁰Harvey, J. K., "Some Measurements on a Yawed Slender Delta Wing with Leading Edge Separation," Aeronautical Research Council, R&M 3160, Oct. 1958.
- ¹¹Nelson, R. C., "Unsteady Aerodynamics of Delta Wings," AGARD R-776, April 1991.
- ¹²Carcaillet, R., Manie, F., Pagan, D., and Solignac, J. L., "Leading Edge Vortex Flow over a 75 degree Swept Delta Wing—Experimental and Computational Results," International Council of the Aeronautical Sciences, ICAS-86-1.5.1, Sept. 1986.
- ¹³Ornberg, T., "A Note on the Flow Around Delta Wings," Royal Inst. of Technology, Stockholm, Sweden, Rept. KTH-AERO TN38, Feb. 1950.
- ¹⁴Peckham, D. H., "Low-Speed Wind-Tunnel Tests on a Series of Uncambered Slender Pointed Wings with Sharp Edges," Aeronautical Research Council, R&M 3186, Dec. 1958.
- ¹⁵Roos, F. W., and Kegelman, J. T., "An Experimental Investigation of Sweep Angle Influence on Delta Wing Flows," AIAA Paper 90-0383, Jan. 1990.
- ¹⁶Richwine, D. M., and Fisher, D. F., "In-Flight Leading-Edge Extension Vortex Flow-Field Survey Measurements on a F-18 Aircraft at High Angle of Attack," AIAA Paper 91-3248, Sept. 1991.
- ¹⁷Fink, P. T., and Taylor, J., "Some Early Experiments on Vortex Separation," Aeronautical Research Council, R&M 3489, 1967.
- ¹⁸Stahl, W., Hartmann, K., and Schneider, W., "Force and Pressure Measurements on a Slender Delta Wing at Transonic Speeds and Varying Reynolds Numbers," AGARD CP-83, Paper 9, April 1971.
- ¹⁹Hemsch, M. J., and Luckring, J. M., "Connection Between Leading-Edge Sweep, Vortex Lift and Vortex Strength for Delta Wings," *Journal of Aircraft*, Vol. 27, No. 5, May 1990, pp. 473-475.
- ²⁰Hummel, D., "Research on Vortex Breakdown on Slender Delta Wings," Aircraft Research Association Library Translation No. 12, Oct. 1965.
- ²¹Lambourne, N. C., and Bryer, D. W., "The Bursting of Leading Edge Vortices—Some Observations and Discussion of the Phenomenon," Aeronautical Research Council, R&M 3282, April 1961.
- ²²Hall, M. H., "The Structure of Concentrated Vortex Cores," *Progress in Aeronautical Sciences*, Vol. 7, 1964, pp. 53-110.
- ²³Wedemeyer, E., "Vortex Breakdown," AGARD LS-121, Dec. 1982.
- ²⁴Ashenberg, J., "A Model for Vortex Breakdown on Slender Wings," *AIAA Journal*, Vol. 25, No. 12, Dec. 1987, pp. 1622-1624.
- ²⁵Erickson, G. E., "Flow Studies of Slender Wing Vortices," AIAA Paper 80-1423, July 1980.
- ²⁶Kegelman, J., and Roos, F., "Effects of Leading Edge Shape and Vortex Burst on the Flowfield of a 70° Sweep Delta Wing," AIAA Paper 89-0086, Jan. 1989.